Supplement of Hydrol. Earth Syst. Sci., 26, 2561–2582, 2022
https://doi.org/10.5194/hess-26-2561-2022-supplement

Hydrology and Earth System Sciences
Open Access

Supplement of

Influences of land use changes on the dynamics of water quantity and quality in the German lowland catchment of the Stör

Chaogui Lei et al.

Correspondence to: Chaogui Lei (cglei@hydrology.uni-kiel.de)

Supplement

Text S1. Definition of the performance metrics applied in SWAT model

Kling–Gupta efficiency (KGE) is based on the decomposition of the NSE and the mean square error into three components: correlation, variability error, and bias error (Gupta et al., 2009). KGE uses the Euclidian distance to combine these three components, as shown in formula (1). It ranges from $-\infty$ to 1, where 1 indicates the optimum model performance.

Nash-Sutcliffe efficiency (NSE) is a normalized statistic that assesses the magnitude of the residual variance relative to the measured data variance (Nash and Sutcliffe, 1970). It is calculated using formula (2), obtaining a range from $-\infty$ to 1. A value closer to 1 indicates a better performance. A value of 0 corresponds to the arithmetic mean of the observed data.

Percent bias (PBIAS) determines if the average of the simulated data is larger or smaller than the corresponding observed values (Gupta et al., 1999). Zero is the optimal value for PBIAS. In this study, positive values indicate overestimation of the observed values by the model, while negative values indicate underestimation by the model. PBIAS is calculated with formula (3).

RSR is the ratio of standard deviation of the observed data (STDEV) and the Root mean square error (RMSE) (Singh et al., 2004), as shown in formula (4). It standardizes RMSE using the STDEV.

$$\mathrm{KGE} = 1 - \sqrt{(r-1)^2 + \left(\frac{Q_i^{sim}}{Q_i^{ob}} - 1\right)^2 + \left(\frac{\overline{Q}^{sim}}{\overline{Q}^{ob}} - 1\right)^2} \qquad (1)$$

$$\mathrm{NSE} = 1 - \frac{\sum_{i=1}^{n}\left(Q_i^{ob} - Q_i^{sim}\right)^2}{\sum_{i=1}^{n}\left(Q_i^{ob} - \overline{Q}^{ob}\right)^2} \qquad (2)$$

$$\mathrm{PBIAS} = \frac{\sum_{i=1}^{n}\left(Q_i^{sim} - Q_i^{ob}\right)}{\sum_{i=1}^{n} Q_i^{ob}} \times 100 \qquad (3)$$

$$RSR = \frac{\sqrt{\sum_{i=1}^{n}\left(Q_i{}^{ob} - Q_i{}^{sim}\right)^2}}{\sqrt{\sum_{i=1}^{n}\left(Q_i{}^{ob} - \bar{Q}^{ob}\right)^2}} \qquad (4)$$

where r is the linear correlation coefficient between simulated and model values; $Q_i{}^{sim}$ is the simulated value; $Q_i{}^{ob}$ is the observed value; $\bar{Q}^{sim}$ and $\bar{Q}^{ob}$ are the respective arithmetic mean of simulated and observed values; n is the number of data records.

Table S1. Parameters used to calibrate streamflow, sediment, total phosphorus and total nitrogen.

Parameters	Definition	Calibrated range			Calibrated value		
Parameters used to calibrate streamflow							
		WILL	SAR	PAD	WILL	SAR	PAD
r_SURLAG	Surface runoff lag coefficient	0.1-0.6	0.1-0.6	0.1-0.5	0.13	0.13	0.13
r_GWDELAY*fs*	Groundwater delay time – fast shallow aquifer (days)	48-85	40-80	65-100	83	42	71
r_ALPHABF*fsh*	Baseflow alpha factor – fast shallow aquifer (day^{-1})	0.17-0.38	0.18-0.38	0.05-0.22	0.18	0.26	0.08
r_RCHRG*ssh*	Aquifer percolation fraction – slow shallow aquifer	0.8-0.94	0.08-0.58	0.38-0.7	0.91	0.34	0.44
r_GWDELAY*ss*	Groundwater delay time – slow shallow aquifer (days)	68-105	58-100	80-120	80	92	87
r_ALPHABF*ssh*	Baseflow alpha factor – slow shallow aquifer (day^{-1})	0.0009-0.002	0.001-0.007	0.003-0.009	0.0019	0.0036	0.0064
r_RCHRG*dp*	Aquifer percolation fraction inactive deep aquifer	0.02-0.15	0.015-0.14	0.1-0.45	0.14	0.03	0.15
r_ESCO	Soil evaporation compensation factor	0.85-0.98	0.93-1	0.7-0.95	0.86	0.94	0.77
r_EPCO	Plant uptake compensation factor	0.01-0.025	0.05-0.22	0.1-0.35	0.02	0.06	0.23
as_CN2	Initial SCS runoff curve number for moisture condition II	-13 - -1	-12 - -1	-12 - -2	-5.64	-3.27	-4.89
as_SOL_AWC	Available water capacity of the soil layer (mm)	-0.06 - 0.02	-0.06 - -0.01	-0.04 - 0.03	-0.006	-0.020	0.001
m_SOL_K	Saturated hydraulic conductivity (mm h^{-1})	0.7-1.3	0.8-1.2	0.8-1.2	1.052	0.811	1.079
Parameters used to calibrate sediment							
r_ADJ_PKR	Peak rate adjustment factor for sediment routing in the main channel	0.55-2			0.61		
r_CH_COV_1	Channel erodibility factor	0.1-0.5			0.41		
r_CH_COV_2	Channel cover factor	0.4-0.7			0.57		
r_USLE_P	USLE support practice factor	0.5-1			0.93		
m_SLSUBBSN	Average slope length (m)	0.8-1.08			0.88		
m_HRUSLP	Average slope stepness (m m^{-1})	0.95-1.28			1.1		
r_LAT_SED	Sediment concentration in lateral and groundwater flow (mg l^{-1})	55-140			110		
r_USLE_K	Soil erodibility (K) factor	0.06-0.2			0.09		
as_SOL_Z	Depth from soil surface to bottom of layer (mm)	-70-20			-65		
r_USLE_C	Minimum value of USLE C factor for land cover/plant	0.08-0.43 (cropland); 0.002-0.017 (pasture)			0.192 (cropland), 0.015 (pasture)		
Parameters used to calibrate total phosphorus							
r_P_UPDIS	Phosphorus uptake distribution parameter	30-100			73.61		
r_PPERCO	Phosphorus percolation coefficient	10-16			10.3		
r_PHOSKD	Phosphorus soil partitioning coefficient	115-190			181.14		
r_PSP	Phosphorus sorption coefficient	0.01-0.5			0.21		
r_ERORGP	Organic P enrichment ratio	0.8-4.8			2.38		
r_GWSOLP	Concentration of soluble phosphorus in groundwater contribution to stream flow from the subbasin	0.04-0.4			0.19		
r_SOL_SOLP	Soluble phosphorus concentration in the soil layer (mg kg^{-1})	30-90			32.1		
Parameters used to calibrate total nitrogen							
r_CMN	Rate factor for humus mineralization of active organic nitrogen	0.001-0.003			0.002		
r_RCN	Concentration of nitrogen in rainfall (mg l^{-1})	1.3-6			5		
r_CDN	Denitrification exponential rate coefficient	0.09-0.18			0.16		
r_N_UPDIS	Nitrogen uptake distribution parameter	20-90			69.05		
r_NPERCO	Nitrogen percolation coefficient	0.03-0.5			0.06		
r_SDNCO	Denitrification threshold water content	0.3-0.95			0.95		
r_HLIFENGW*fsh*	Half-life of nitrate in fast shallow aquifer (days)	30-125			52		
r_HLIFENGW*ssh*	Half-life of nitrate in slow aquifer (days)	250-480			454		
r_SHALLSTN*ssh*	Initial concentration of nitrate in slow aquifer (mg l^{-1})	30-85			37.41		

Note: for calibration, the parameter values were varied by replacing (r), multiplication (m) or addition/subtraction (as)

Text S2. Calculation of the changes in land use indicators and water quantity and quality variables

The absolute change in each land use indicator is derived using the following equations:

$$P_{ij1} = P_{ij2010} - P_{ij1987} \quad (5)$$

$$P_{ij2} = P_{ij2019} - P_{ij2010} \quad (6)$$

$$P_{ij3} = P_{ij2019} - P_{ij1987} \quad (7)$$

where, *i* is one certain land use indicator, *j* is the subbasin number, P_{ij1987}, P_{ij2010}, P_{ij2019} indicate the value of indicator *i* in subbasin *j* in 1987, 2010, and 2019, respectively. P_{ij1}, P_{ij2}, and P_{ij3} indicate the absolute changes in indicator *i* in the subbasin *j* during periods 1987-2010, 2019-2010, and 1987-2019, respectively. These are used as predicator variables in the PLSR approach (see S3).

The absolute change in each water quantity and quality variable is computed using the following equations:

$$R_{kj1} = R_{kj2010} - R_{kj1987} \quad (8)$$

$$R_{kj2} = R_{kj2019} - R_{kj2010} \quad (9)$$

$$R_{kj3} = R_{kj2019} - R_{kj1987} \quad (10)$$

where *k* is the water quantity and quality variable, R_{kj1987}, R_{kj2010}, and R_{kj2010} are the respective mean annual values of variable *k* in subbasin *j* during the simulation of 1990-2019 under the land use condition of 1987, 2010, and 2019, respectively. Changes in the water quantity and quality variables due to respective land use change from 1987 to 2010, from 2010 to 2019, or from 1987 to 2019 are depicted by R_{kj1}, R_{kj2}, and R_{kj3}, respectively, which are referred as changes of 1987-2010, 2010-2019, and 1987-2019 in Figure 5 in the paper. These are used as the response variables in the PLSR approach (see S3).

Text S3. Description of predictors, response variables and cross-validation of PLSR

Predictors: The absolute changes in each of the 24 land use indicators involving arable (*a*), pasture (*p*), urban(*u*), and forest (*f*) areas, which include area percent (PLAND*a*, PLAND*p*, PLAND*u*, and PLAND*f*), largest patch index (LPI*a*, LPI*p*, LPI*u*, and LPI*f*), shape index (AWMSI*a*, AWMSI*p*, AWMSI*u*, and AWMSI*f*), aggregation index (AI*a*, AI*p*, AI*u*, and AI*f*), contiguity index (CONTIGAW*a*, CONTIGAW*p*, CONTIGAW*u*, and CONTIGAW*f*), and interspersion index (IJI*a*, IJI*p*, IJI*u*, and IJI*f*), see Figure S1. The changes are calculated for the three periods 1987-2010, 2010-2019, and 1987-2019.

Response variables: The absolute changes in each one of the 7 water quantity and quality variables incl. ET, SQ, BF, WYLD, SED, TP, and TN. Each of them is calculated by the differences between two simulations with different land use maps (scenarios), see also Text S2.

Cross-validation method: We used the Repeat k-Fold Cross-validation method, which is a commonly used method to achieve a balanced estimate of PLSR model performance. Specifically, we used “50 random repetitions on 10 equal segments”. For example, a dataset of 60 observations will be randomly split into 10 equal segments (one segment has 6 observations) for 50 times. For each of these 50 random repetitions, the model will be run for each segment and return a performance score. The mean model performance score is calculated as the mean of the performance scores for the 10 segments and 50 repetitions, i.e., averaging 500 performance scores. This value is used to assess the final performance of cross-validation.

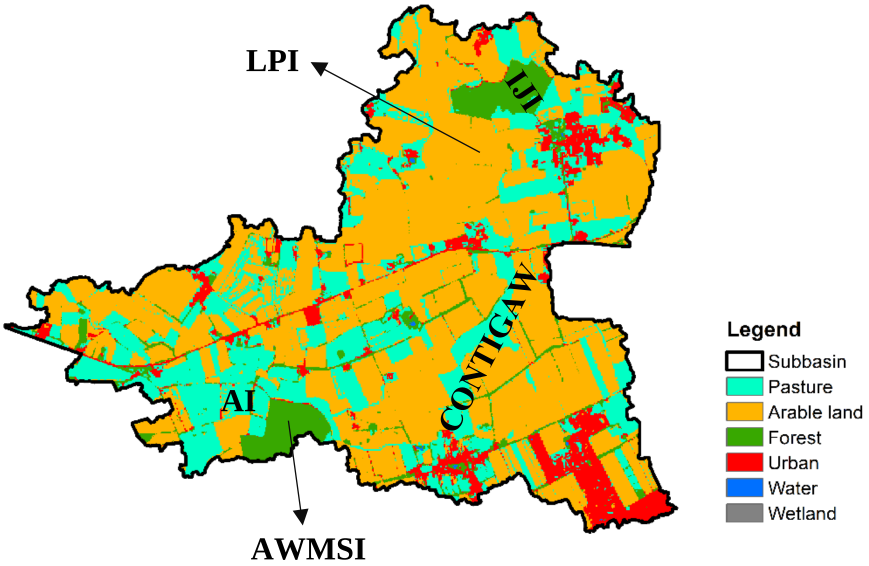

Figure S1. Sketch illustrating the landscape configuration metrics used in this study

References

Gupta, H. V., Sorooshian, S., and Yapo, P. O.: Status of automatic calibration for hydrologic models: Comparison with multilevel expert calibration, J. Hydrol. Eng., 4, 135-143, https://doi.org/10.1061/(ASCE)1084-0699(1999)4:2(135), 1999.

Gupta, H. V., Kling, H., Yilmaz, K. K., and Martinez, G. F.: Decomposition of the mean squared error and NSE performance criteria: Implications for improving hydrological modelling, J. Hydrol., 377, 80-91, https://doi.org/10.1016/j.jhydrol.2009.08.003, 2009.

Nash, J. E. and Sutcliffe, J. V.: River flow forecasting through conceptual models part I—A discussion of principles, J. Hydrol., 10, 282-290, https://doi.org/10.1016/0022-1694(70)90255-6 , 1970.

Singh, J., Knapp, H., and Demissie, M.: Hydrologic modeling of the Iroquois River watershed using HSPF and SWAT, J. Am. Water Resour. Assoc., 41, 343-360, https://doi.org/10.1111/j.1752-1688.2005.tb03740.x, 2005.